Journal of Molecular Structure 1216 (2020) 128277

Contents lists available at ScienceDirect

Journal of Molecular Structure

journal homepage: http://www.elsevier.com/locate/molstruc

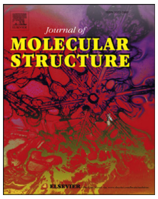

Dipole forbidden, nuclear electric quadrupole allowed transitions and chirality: The broadband microwave spectrum and structure of 2-bromo-1,1,1,2-tetrafluoroethane

Joshua E. Isert [a], Frank E. Marshall [a], William C. Bailey [b], G.S. Grubbs [a, *]

[a] Department of Chemistry, Missouri University of Science and Technology, 104 Schrenk Hall, 400 W. 11th St., Rolla, MO, 65409, USA
[b] Kean University (Retired), Chemistry-Physics Department, 1000 Morris Avenue, Union, NJ, 07080, USA

ARTICLE INFO

Article history:
Received 31 December 2019
Received in revised form
26 March 2020
Accepted 14 April 2020
Available online 28 April 2020

Keywords:
Chirality
Dipole forbidden transitions
Rotational spectroscopy
Structure determination methods
CP-FTMW

ABSTRACT

The chirped pulse Fourier transform microwave spectrum of the chiral molecule 2-bromo-1,1,1,2-tetrafluoroethane has been observed in the 6–18 GHz region of the electromagnetic spectrum and is reported. Six isotopologues, including ^{13}C isotopic substitution at each carbon atom in both the ^{79}Br and ^{81}Br parent species have been observed in natural abundance. All rotational constants, quartic centrifugal distortion contants, and nuclear quadrupole coupling tensor components have been experimentally determined and have been reported. In addition, spin-rotation components M_{aa}, M_{bb}, and M_{cc} are also determined and reported. The theoretical structure of the species has been determined and reported. The C–C–Br backbone structure has been determined experimentally implementing both Kraitchman single and Rudolph double substitution analysis, the later being explained in the text. 3440 transitions total have been observed with 45 transitions being electric dipole forbidden. These dipole forbidden transitions have been identified as they are planned to be used in microwave three-wave mixing experiments in order to better understand their role, if any, in determining chirality. The determined nuclear electric quadrupole coupling tensor has been diagonalized and compared to similar small alkane species in order to make inferences on the effects of fluorination on the C–Br bond.

1. Introduction

In 2013, Patterson, Schnell, and Doyle introduced a new and powerful technique to differentiate between enantiomeric species using a series of imposed electric fields [1]. The experiment leveraged the idea that a chiral molecule, by symmetry, must have a nonzero permanent electric dipole moment components along all three axes of a molecule in the principal axis system (PAS). Furthermore, this chirality condition also requires one of these three components be opposite in sign amongst the enantiomeric pair. The experiment was carried out, then, by imposing orthogonally oriented electric fields on the molecules that aligned with the two of the electric-dipole allowed transition types. The transition system was picked so that there would be a required relaxation in the third (also orthogonal) electric dipole moment component, creating a 3-state loop. An example of this loop is in Fig. 1. Because the sign product of the three-state scheme is exactly opposite between the enantiomeric pair, chiral species could be qualitatively and quantitatively determined as the free induction decays would be exactly π (180°) out-of-phase with one another. This experiment was later made so that it could be extended to more traditional chirped pulse, Fourier transform microwave (CP-FTMW) spectrometers by Pate [2], Schnell [3], and Patterson [4]. This has become known as the microwave three-wave mixing (M3WM) experiment.

In 2009, Grubbs and Cooke began a series of studies investigating electric dipole forbidden, quadrupole allowed transitions [5–11]. These transitions occurred when atoms containing large nuclear quadrupole moments (like Br or I) were combined with comparatively small or approximately equal size rotational constants. First theorized by Javan [12] and observed by Oka [13], these forbidden transition pathways are made through an off-diagonal nuclear electric quadrupole coupling tensor component. The electric dipole forbidden transition arises from a three-state system in which the electric dipole forbidden transition type and the electric dipole allowed transition type are linked by the χ tensor off-

---

* Corresponding author.
E-mail address: grubbsg@mst.edu (G.S. Grubbs).

https://doi.org/10.1016/j.molstruc.2020.128277

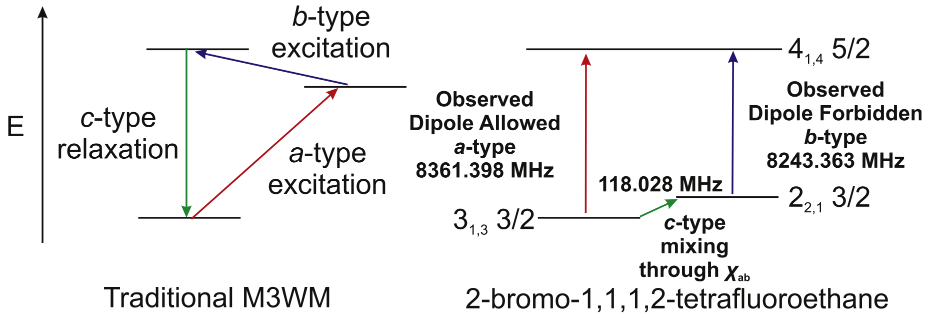

Fig. 1. Example of the 3-state excitation/relaxation pattern of a microwave three-wave mixing M3WM experiment and an electric-dipole forbidden transition in 2-bromo-1,1,1,2-tetrafluoroethane. The transition pathway for M3WM shown is *a*- and *b*-type excitation with a *c*-type relaxation, but any orthogonal combination can be, in theory, utilized. For the dipole forbidden transition, the transition arises from the large χ_{ab} off-diagonal component. In this scenario, the states that mix are linked by a *c*-type transition. There is an observed, allowed *a*-type transition in conjunction with the observed, forbidden *b*-type transition.

diagonal component in question (an *a*-type and *b*-type transition are linked by χ_{ab}). The mixing of states is done via the third electric dipole allowed transition type not contained in the off-diagonal component. An example of this is if the forbidden and allowed transition are *b*-type and *a*-type, respectively, then the mixing states are connected by a *c*-type linkage and the off-diagonal nuclear electric quadrupole tensor component providing for the mixing is χ_{ab} as shown for one of the title molecule transitions in Fig. 1. In 2016, we extended these findings by studying the molecule bromoperfluoroacetone which had multiple large off-diagonal nuclear quadrupole coupling tensor components which provided for the observation of rare *x*-type transitions [9]. *x*-type transitions are defined as transitions that do not have a change in parity in either the K_a or K_c quantum state values. These transitions, in turn, are not explicitly linked to any electric dipole moment component.

These two seemingly different areas of study, though, have so many interesting areas of overlap in their application that the authors were curious as to the application of M3WM to a chiral molecule that exhibited nuclear quadrupole allowed, electric dipole forbidden transitions. In order to study this, however, a test molecule that possessed all of the required properties-chirality, a large quadrupolar nucleus with large off-diagonal tensor components, and rotational constants on the order of these tensor components-needed to be studied and fully understood spectroscopically and structurally by traditional microwave rotational spectroscopy techniques. Then, this molecule can be isolated for forbidden transitions of importance and studied in a M3WM experiment.

In this manuscript, therefore, we report the first part of these experiments by presenting the CP-FTMW spectral and structural analysis of the title molecule, 2-bromo-1,1,1,2-tetrafluoroethane. Along with this being the first known report of 2-bromo-1,1,1,2-tetrafluoroethane's rotational spectrum and analysis, we also identify potential forbidden transition targets of this molecule that will be tested in the subsequent M3WM experiments.

2. Experiment

Rotational spectroscopic measurements were made with the CP-FTMW spectrometer located at Missouri S&T. The spectrometer has been detailed elsewhere in the literature.[9,14] These experiments obtained spectra in the 6–18 GHz frequency range utilizing two separate 6 GHz broadband regions (6–12 and 12–18 GHz). Chirp excitation widths were set to 4 μs. These experiments utilized the spectrometer's traditional supersonic sampling method for gases with a Parker-Hannifin Series 9 solenoid valve with 0.8 mm orifice. 97% pure 2-bromo-1,1,1,2-tetrafluoroethane was purchased from SynQuest Laboratories® and used without further purification. From this sample, a 3% gas mixture in industrial grade Ar was prepared. The gas mix was then introduced into the spectrometer at a backing pressure of 0.67 atm (absolute pressure). The spectrometer operated at a 5 Hz valve rate with 5 free induction decays (FIDs) being collected with each gas pulse. Each region was averaged for 2.5 million FIDs and Fourier transformed using Kisiel's FFTS [15] software with a Bartlett window. 2.5 million averages represents approximately 2.5 days of averaging for the instrument. Linewidths for these experiments were approximately 60–80 kHz. The resultant spectrum from the 6–12 GHz region is presented in Fig. 2.

3. Quantum chemical calculations

Quantum chemical calculations were performed in order to arrive at accurate equilibrium geometric structures and ^{79}Br and ^{81}Br nuclear quadrupole coupling constants in order to assist with assignment of the transitions belonging to 2-bromo-1,1,1,2-tetrafluoroethane in the resultant experimental microwave spectrum. All quantum chemical calculations were performed using the Gaussian09® program suite [16].

Geometry optimization was used for the components of the NQCC tensor χ_{ij} and are related to those of the electric field gradient tensor q_{ij} by

$$\chi_{ij}(\mathrm{MHz}) = (eQ/h) \times q_{ij}(\mathrm{a.u.}) \tag{1}$$

where *e* is the fundamental electric charge, *Q* is the electric quadrupole moment of the nucleus in question, and *h* is Plancks constant. The coefficient eQ/h is taken as a best-fit parameter determined by linear regression analysis of calculated q_{ij} on the experimental structures of a number of molecules versus experimental υ_{ij}. The premise that underlies this procedure is that errors inherent in the computational model as well as zero-point vibrations and relativistic effects are systematic and can be corrected, as least partially, by the best-fit coefficient eQ/h.

For bromine, the recommended model for calculation of theq_{ij} is B1LYP/TZV (3df,3p) [17]. Here, B1LYP is Beckes one-parameter method with Lee-Yang-Parr correlation as implemented by Adamo and Barone [18,19]. TZV are Ahlrichs bases [20] augmented here with 3 sets of *d* and one set of *f* polarization functions on heavy atoms, and 3 sets of *p* functions on hydrogens. These polarization functions are those recommended for use with Pople 6-311G bases, and were obtained online from the EMSL basis set library [21,22]. Thus, for conversion of q_{ij} to χ_{ij}, $eQ/h(^{79}\mathrm{Br}) = 77.628(43)$ MHz/a.u. and $eQ/h(^{81}\mathrm{Br}) = 64.853(40)$ MHz/a.u.[17,23] Calculation was made on a molecular structure given by MP2/aug-cc-pVTZ optimization.

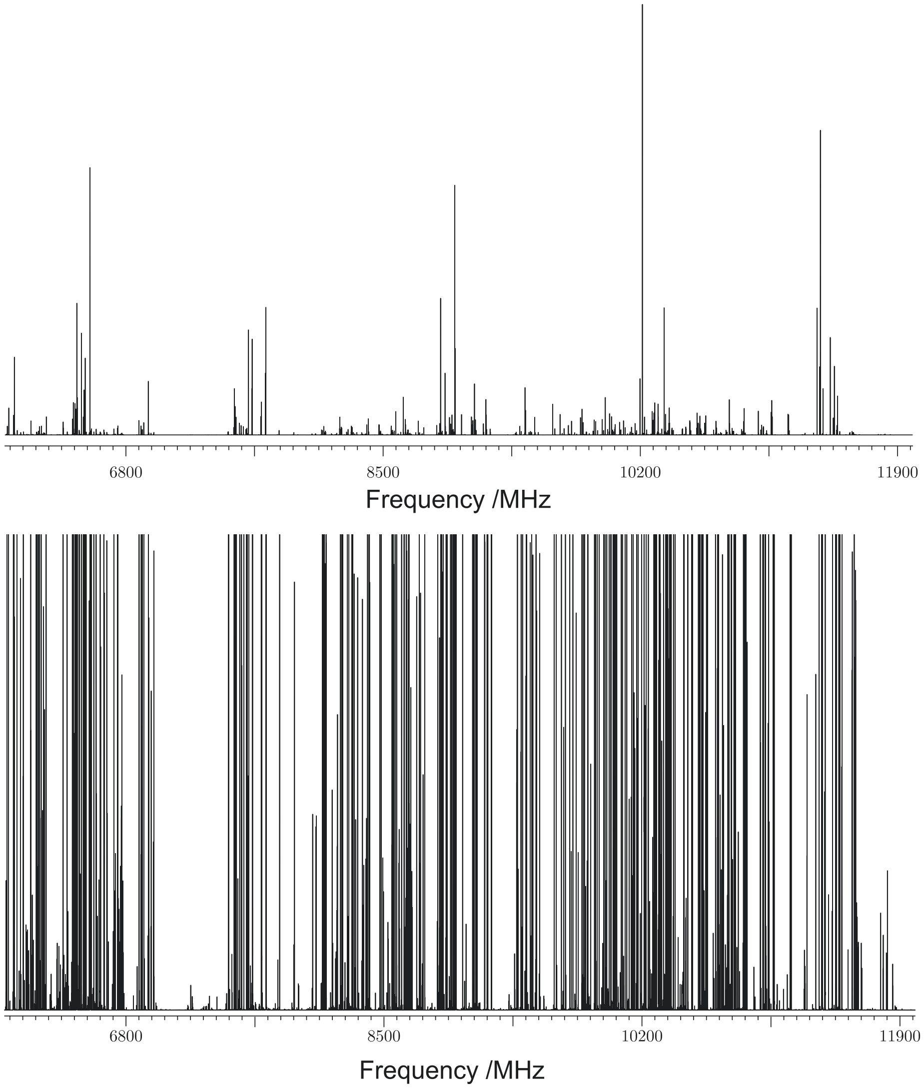

Fig. 2. CP-FTMW spectrum of 2-bromo-1,1,1,2-tetrafluoroethane in the 6–12 GHz frequency region. The top is adjusted so that the y-axis maxes out with the most intense transition. The bottom is a zoom-in of the y-axis to the baseline to show the transition density of the collected spectrum.

Table 1
Quantum Chemical Calculation Parameters for 2-bromo-1,1,1,2-tetrafluoroethane at the MP2/aug-cc-pVTZ level. See text for details of calculation.

Parameter	$C_2H^{79}BrF_4$	$C_2H^{81}BrF_4$
A/MHz	3057.824	3056.798
B/MHz	1173.871	1161.671
C/MHz	1007.598	998.487
χ_{aa} /MHz	400.707	335.753
χ_{bb} /MHz	−153.276	−129.0180
χ_{cc} /MHz	−247.432	−206.735
χ_{ab} /MHz	−308.447	−256.835
χ_{ac} /MHz	217.048	181.450
χ_{bc}/MHz	−85.289	−70.909
η[a]	0.048	0.046
$\|\mu_a\|$[b] /D	0.580	0.580
$\|\mu_b\|$[b] /D	0.020	0.019
$\|\mu_c\|$[b] /D	1.298	1.298

[a] Asymmetry of the diagonalized χ tensor: $\eta = \frac{\chi_{xx} - \chi_{yy}}{\chi_{zz}}$.

[b] Absolute values for the calculated dipole moments have been reported due to chiral nature of the molecule.

These results are shown in Tables 1 and 2 with the predicted equilibrium structure of 2-bromo-1,1,1,2-tetrafluoroethane being presented in Fig. 3.

4. Results and analysis

Quantum chemical calculations provided an excellent starting point for transition assignment. The resultant spectral transition density is high with an approximate value of one assigned transition per 5 MHz of recorded spectra. This density, however, was not as problematic as the similar molecule *trans*-3-Bromo-1,1,1,2,2-pentafluoropropane due to very few possible low energy conformations [10]. The optimized structure presented in the previous section is the lowest energy structure for 2-bromo-1,1,1,2-tetrafluoroethane and the most intense spectra presented in Fig. 2 correspond to the parent ^{79}Br and ^{81}Br isotopologues. The parent spectra contained electric-dipole allowed, *a*-, *b*-, and *c*-type spectra within the *P*-, *Q*-, and *R*-branches. The intensity of the spectra, as shown in Fig. 2, provided for the observation of the ^{13}C isotopologue of each the ^{79}Br and ^{81}Br species in natural abundance with C_1 being denoted the position next to the Br and C_2 being the remaining carbon.

Table 2
Atomic Coordinates for 2-bromo-1,1,1,2-tetrafluoroethane from structural optimization at the MP2/aug-cc-pVTZ level or theory (all units are in Å).

$C_2H^{79}BrF_4$

Atom	*a*	*b*	*c*
Br	1.512488	−0.168903	0.003316
C_1	−0.150583	0.616410	−0.505440
C_2	−1.322034	−0.228673	−0.009840
H	−0.181057	0.673229	−1.590280
F	−0.269074	1.861683	0.024236
F	−1.277692	−1.445319	−0.557779
F	−1.329046	−0.350556	1.313482
F	−2.467221	0.355186	−0.383886

$C_2H^{81}BrF_4$

Atom	*a*	*b*	*c*
Br	1.496186	−0.164248	0.003234
C_1	−0.168366	0.617959	−0.505462
C_2	−1.338219	−0.229323	−0.009841
H	−0.198977	0.674737	−1.590300
F	−0.289172	1.863000	0.024237
F	−1.291616	−1.445876	−0.557800
F	−1.344964	−0.351239	1.313480
F	−2.484508	0.352397	−0.383844

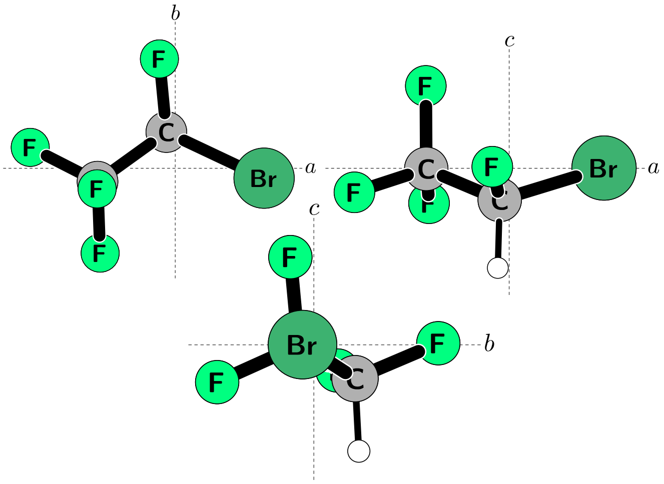

Fig. 3. Equilibrium structure of 2-bromo-1,1,1,2-tetrafluoroethane in the *ab*, *ac*, and *bc* planes of the principal axis system.

Spectra were assigned using Pickett's SPFIT/SPCAT program suite [24] with Kisiel's AABS package [25], available from the PROSPE website [26,27], used as a front-end in order to visually observe predicted transition patterns and expedite transition assignment. An uncertainty of 10 kHz was attributed to line centers. Once the dipole allowed transitions were assigned, then the authors went back and assigned dipole forbidden transitions. In total, 3440 transitions were assigned with obs-calc residuals less than or equal to 3σ of the line center uncertainty. Spectra were fit using a Watson's S-reduced Hamiltonian [28] in the I^r representation. All quartic centrifugal distortion constants were determined along with the entire nuclear quadrupole coupling tensor arising from the bromine nucleus. Spin-rotation components M_{aa}, M_{bb}, and M_{cc} were also determined. A complete list of all assigned transitions and fits can be found in the Supplemental Material while the spectroscopic parameters are presented in Table 3.

5. Discussion

2-bromo-1,1,1,2-tetrafluoroethane provides for interesting electronic and geometric structural studies as it fits into a host of previously studied similarly fluorinated and brominated alkanes [9–11,11,29–31,31–40]. In order to better understand this structure, then, and compare it to the known experimental works and the theoretical structure presented in this work, the geometric structure is presented in the *Structure of 2-bromo-1,1,1,2-tetrafluoroethane* subsection while electronic structural arguments and comparisons are made in the following *Nuclear Quadrupole Coupling Tensor Comparisons* subsection. The last subsection, *Electric Dipole Forbidden, Quadrupole Allowed Transitions*, discusses the observed dipole forbidden, quadrupole allowed transitions as they will be utilized in the next set of experiments toward testing new ways to possibly probe and understand chiral molecules.

5.1. Structure of 2-bromo-1,1,1,2-tetrafluoroethane

Rotational analysis of the carbon and bromine isotopologues provides an opportunity to compare some experimentally determined atomic positions to the theoretical equilibrium structure. The atomic positions for the calculated ^{79}Br and ^{81}Br species are presented in Table 2. To make this comparison, Kraitchman single substitution structures were performed using the ^{79}Br and ^{81}Br each as the parent species in the KRA program found on Kisiel's PROSPE website [26]. The results of these calculations are presented in Table 4. As is presented in the table, using ^{79}Br as the parent species produced an imaginary number for the *a*-coordinate in the C_1 position. This changes the coordinate's value by almost 0.1 Å from the experimentally determined ^{81}Br and theoretical *a*-coordinate value. Comparisons of the Bromine, C_3 and remaining coordinates for all other atomic postitions were in good agreement with thereotical and experimentally determined values.

To understand the effect this difference had, then, we performed a geometry evaluation of these positions using the EVAL program also available on Kisiel's PROSPE website [26]. The results are presented in Table 5. Using only the Kraitchman substitution values for ^{79}Br, ∠CCBr and the C−C bond length is relatively unaffected by the difference in the *a*-coordinate, but the C−Br bond length is significantly different being well outside uncertainty predictions - 1.783(4)Å for ^{79}Br vs. 1.852(14)Å for ^{81}Br.

Table 3
Microwave spectroscopic parameters of 2-bromo-1,1,1,2-tetrafluoroethane.

Parameter	$C_2H^{79}BrF_4$	$^{13}CH^{79}BrFCF_3$	$CH^{79}BrF^{13}CF_3$	$C_2H^{81}BrF_4$	$^{13}CH^{81}BrFCF_3$	$CH^{81}BrF^{13}CF_3$
A/MHz	3063.0485(1)[a]	3051.3905(4)	3062.3324(4)	3062.0101(1)	3050.3339(5)	3061.0434(8)
B/MHz	1163.59326(6)	1162.9334(1)	1158.9444(1)	1151.48435(5)	1150.8618(2)	1146.7504(2)
C/MHz	1000.20122(5)	999.4611(1)	996.6689(1)	991.13102(5)	990.3293(1)	987.5148(2)
D_J /kHz	0.1114(2)	0.1111(6)	0.1103(5)	0.1088(1)	0.1069(6)	0.1082(7)
D_{JK} /kHz	0.2372(8)	0.240(2)	0.236(2)	0.2341(8)	0.226(3)	0.235(3)
D_K /kHz	0.197(4)	0.203(8)	0.22(1)	0.180(3)	0.15(1)	0.16(2)
d_1 /Hz	−18.61(5)	−19.5(1)	−18.3(1)	−18.06(5)	−18.0(1)	−17.9(2)
d_2 /Hz	2.54(2)	3.03(5)	2.54(6)	2.40(2)	2.15(6)	2.30(6)
χ_{aa} /MHz	399.223(3)	399.413(7)	398.500(7)	334.477(3)	334.487(7)	334.47(2)
χ_{bb} /MHz	−154.542(4)	−153.96(1)	−153.85(1)	−130.067(4)	−130.09(1)	−130.07(3)
χ_{cc} /MHz	−244.682(2)	−245.457(9)	−244.652(9)	−204.411(2)	−204.39(1)	−204.40(2)
χ_{ab} /MHz	−305.54(3)	−305.6(1)	−305.81(9)	−254.35(2)	−254.4(1)	−254.2(1)
χ_{ac} /MHz	−218.56(5)	−218.1(1)	−281.6(1)	−182.72(3)	−183.1(1)	−183.0(2)
χ_{bc} /MHz	85.97(3)	85.3(1)	86.20(9)	71.43(3)	71.3(1)	71.3(3)
M_{aa} /kHz	2.5(3)	[2.5][e]	[2.5]	3.5(2)	[3.5]	[3.5]
M_{bb} /kHz	1.9(1)	[1.9]	[1.9]	1.9(1)	[1.9]	[1.9]
M_{cc}/kHz	2.2(1)	[2.2]	[2.2]	2.2(1)	[2.2]	[2.2]
N[b]/MHz	1246	252	295	1292	203	152
MWσ_{rms}[c] /kHz	10.9	15.9	13.9	10.9	14.7	15.6
σ_{rms}[d]	1.09	1.59	1.39	1.09	1.47	1.56

[a] Numbers in parentheses represent 1σ uncertainty (68% confidence level) and are given in units of the least significant digit.

[b] Number of transitions assigned.

[c] MW σ_{rms} is defined as $\sqrt{(\sum[(\text{obs}-\text{calc})^2]/\text{N})}$.

[d] σ_{rms} is defined as $\frac{\sqrt{(\sum[(\text{obs}-\text{calc})^2]/\text{N})}}{\text{Average}}$ of Attributed Uncertainty.

[e] Numbers in brackets held to determined value of parent (79 or 81) isotopologue.

Table 4
Kraitchman Single Substitution Coordinates [42] for 2-bromo-1,1,1,2-tetrafluoroethane (all units are in Å).

$C_2H^{79}BrF_4$ as Parent			
Atom	a	b	c
Br	1.52023(99)[a,b]	−0.1702(88)	0.00(11)[c]
C_1	−0.097[0.000](21)[d]	0.6153(24)	−0.5032(30)
C_2	−1.3232(11)	−0.2097(72)	0.000(21)
$C_2H^{81}BrF_4$ as Parent			
Atom	a	b	c
Br	1.5038(10)	−0.1655(91)	0.00(12)
C_1	−0.096(16)	0.6350(24)	−0.4796(31)
C_2	−1.3480(11)	−0.2329(64)	−0.000(37)

[a] Numbers in parentheses are the Costain errors [48] and are given in units of the least significant digit.

[b] Kraitchman coordinates do not give sign but attributed signs are from the quantum chemical calculations for purposes of calculating molecular geometries.

[c] Where a value of 0 is given, the Kraitchman calculated coordinate value was imaginary.

[d] Kraitchman single substitution value (in brackets) gives inconsistent structure with isotopologues and calculated structure so double substitution using Rudolph method [41] reported.

Table 5
Experimentally determined structural parameters for 2-bromo-1,1,1,2-tetrafluoroethane.

$C_2H^{79}BrF_4$ as Parent	
Kraitchman Substitution Only	
Parameter	Value
∠CCBr/°	112.3(3)[a]
C−C/Å	1.638(4)
C−Br/Å	1.783(4)
Kraitchman and Rudolph Coordinates Combined	
Parameter	Value
∠CCBr/°	111.8(3)
C−C/Å	1.561(17)
C−Br/Å	1.867(19)
$C_2H^{81}BrF_4$ as Parent	
Parameter	Value
∠CCBr/°	111.4(3)
C−C/Å	1.597(13)
C−Br/Å	1.852(14)

[a] Numbers in parentheses represent 1σ uncertainty (68% confidence level) and are given in units of the least significant digit.

Table 6
Comparison of calculated, Rudolph, r_0, $r_m^{(1)}$, and $r_m^{(2)}$ backbone structural parameters in 2-bromo-1,1,1,2-tetrafluoroethane.

Parameter	r_s^{Rud}	r_0	$r_m^{(1)}$	$r_m^{(2)}$	r_e^{calc}
C−C/Å	1.561(17)[a]	1.5056(20)	1.532(11)	1.546(10)	1.527
C−Br/Å	1.867(19)	1.9479(29)	1.9164(62)	1.9110(55)	1.908
∠CCBr/°	111.8(3)	110.544(72)	111.4(4)	110.8(4)	110.7

[a] Numbers in parentheses represent 1σ uncertainty (68% confidence level) and are given in units of the least significant digit.

Table 7
Second moment analysis for 2-bromo-1,1,1,2-tetrafluoroethane with comparisons to similar molecules.

Species	P_{aa} /uÅ^2	P_{bb} /uÅ^2	P_{cc} /uÅ^2	Reference
$C_2H^{79}BrF_4$	387.305	117.971	47.020	This Work
$C_2H^{81}BrF_4$	391.873	118.027	47.020	This Work
$^{13}CH^{79}BrFCF_3$	387.300	118.350	47.271	This Work
$CH^{79}BrF^{13}CF_3$	388.864	118.203	46.827	This Work
$^{13}CH^{81}BrFCF_3$	391.882	118.431	47.248	This Work
$CH^{81}BrF^{13}CF_3$	393.686	118.081	47.018	This Work
CF_3CF_2Br	391.03	138.355	89.124	[11]
CH_3CH_2Br	129.76	13.7373	3.1384	[29,30]
trans-$CF_3CF_2CH_2Br$	808.32700	107.79201	91.47455	[10]
aa-$CH_3(CH_2)_2CH_2Br$	546.05168	25.70444	6.34108	[31]
ga-$CH_3(CH_2)_2CH_2Br$	406.60396	49.64725	12.01161	[31]
ag-$CH_3(CH_2)_2CH_2Br$	318.91121	54.64829	26.33392	[31]
$CF_3CF_2CF_3$	394.676	166.734	134.339	[32]
g-$CHF_2CF_2CF_3$	356.058	158.203	95.061	[33]
t-$CHF_2CF_2CF_3$	291.404	153.064	135.312	[33]

To give a more accurate picture of the ^{79}Br structure, the authors utilized the double substitution method of Rudolph [41]. As this method is not necessarily standard in today's structure determination methods in microwave rotational spectroscopy, the authors have provided their calculations for this method in the Supplementary Material. A brief explanation of the calculation will be provided here. Although it may be obvious, it is worth noting that, in order to perform the double substitution method, the user needs isotopic substitution data for each substituted position as well as the double substituted isotopologue. For our example, we are trying to find the *a*-coordinate of the C_1 atom of the ^{79}Br species. Therefore, we must have data for the ^{79}Br and ^{81}Br parent species as well as the ^{13}C isotopic data at the C_1 position for each of the parent bromine species giving four total isotopologues sets of data. After all required data is collected, the second moments of all determined isotopologues must be obtained from the determined rotational constants. This was done for all species by using the PLANM program from Kisiel's PROSPE website [26] and is reported in Table 7. From there, the Kraitchman substiution [42] method is the starting point of the procedure utilizing second moments for this determination. For our *a*-coordinate value, we implemented the following equations for C_1 [41]:

$$\Delta P_{aa}^{79/C_1} = \Delta P_{aa}^{13C} - \Delta P_{aa}^{79Parent}$$

$$= \frac{M_{79}\Delta m}{M_{79}+\Delta m} \cdot \frac{\left(P_{bb}^{79Parent} - P_{aa}^{79Parent}\right)\left(P_{cc}^{79Parent} - P_{aa}^{79Parent}\right)}{\left(P_{bb}^{13C} - P_{aa}^{79Parent}\right)\left(P_{cc}^{13C} - P_{aa}^{79Parent}\right)} \cdot a_{79/C_1}^2$$

$$\equiv k a_{79/C_1}^2 \tag{2}$$

$$\Delta P_{aa}^{81/C_1} = \Delta P_{aa}^{13C} - \Delta P_{aa}^{81Parent}$$

$$= \frac{M_{81}\Delta m}{M_{81}+\Delta m} \cdot \frac{\left(P_{bb}^{81Parent} - P_{aa}^{81Parent}\right)\left(P_{cc}^{81Parent} - P_{aa}^{81Parent}\right)}{\left(P_{bb}^{13C} - P_{aa}^{81Parent}\right)\left(P_{cc}^{13C} - P_{aa}^{81Parent}\right)} \cdot a_{81/C_1}^2$$

$$\equiv k' a'^2_{81/C_1} \tag{3}$$

$$\Delta P_{aa}^{81/C_1} - \Delta P_{aa}^{79/C_1} = k' a'^2_{81/C_1} - k a_{79/C_1}^2 \tag{4}$$

$$\left|a_{79/C_1}\right| = \sqrt{\frac{\left(\Delta P_{aa}^{81/C_1} - \Delta P_{aa}^{79/C_1}\right) - k' a'^2_{81/C_1}}{-k}} \tag{5}$$

where the appropriate values have been denoted, *M* stands for the mass of the parent species, and Δm corresponds to the mass difference between the isotopologue and the parent isotope in question. Changing the required coordinate only means changing the required second moment values appropriately. As shown, this method only gives an absolute value coordinate, so any coordinate values with a sign component have to lean on computational coordinates as the Kraitchman method requires. Using this method, it was determined that the *a*-coordinate for the C_1 of the ^{79}Br species is −0.097(21) also using the Costain errors as reported in Table 4. Using this new coordinate, all experimentally determinable parameters for the ^{79}Br and ^{81}Br structures are in agreement. See Table 5.

Being that Rudolph's method is not a common method for implementing multiple substitution species, it is important to put it in context and compare with other semi-empirical methods as well as our calculated r_e structure. The major difference between these methods and Rudolph's method is that Rudolph's method is entirely empirical. In this way, it is very much like Kraitchman's method. In fact, the single substitution formulae within the calculation are the same as Kraitchman's method [41]. In this way, the only assumption that is made is that isotopic substitution is not changing the interaction potential. Common methods like r_0, $r_m^{(1)}$, and $r_m^{(2)}$ require empirical starting points [43]. To show this and compare, calculations for the r_0, $r_m^{(1)}$, and $r_m^{(2)}$ structures were performed in Kisiel's STRFIT [44] and are reported in Table 6. The output files from these fits are also supplied in the Supplemental Material. When the molecule is underdetermined, the semi-empirical structure relies much more heavily on the input calculation. In our case, the *c* and *d* constants typical of the $r_m^{(1)}$ and $r_m^{(2)}$ are not well determined. Although all determined structural parameter methods are in good agreement with the theoretical structure presented in Table 6, the best agreement in the semi-empirical methods seems to be with $r_m^{(2)}$. However, the general trend in these semi-empirical approaches is that the values are also better aligning with Rudolph's values, so it is unclear if further empirical data not provided in this study would move the semi-empirical more toward the Rudolph value or stay closer to the calculated r_e structure.

As a second experimental confirmation of the structure, the second moment method of Bohn was used [45]. For this, the second moment values for the title molecule are reported in Table 7 and compared to similar known molecular studies. If the structure presented in Fig. 3 is the assumed experimental structure then, according to Bohn's method, the CF_3 group should contribute approximately 45 μÅ^2 to P_{cc}. The fluorine on the C_1 atom is calculated to be very close to the *ab*-plane, therefore, it will not have a contribution to the P_{cc} value, so themate contribution of the H atom, according to its calculated contribution is 2.5 μÅ^2. This is in very good agreement with the reported value of 47.020 μÅ^2. All reported fluorinated species with or without the bromine seem to follow this trend, so there is no evidence to suggest that this

Table 8
Bromine-centered χ tensor values for all isotopologues of 2-bromo-1,1,1,2-tetrafluoroethane.

Species	χ_{zz} /MHz	χ_{xx} /MHz	χ_{yy} /MHz	η[a]
$C_2H^{79}BrF_4$	599.88(3)[b]	−286.11(3)	−313.77(4)	0.04611(8)
$C_2H^{81}BrF_4$	501.11(2)	−238.97(2)	−262.14(2)	0.04623(7)
$^{13}CH^{79}BrFCF_3$	599.74(9)	−285.42(8)	−314.32(8)	0.0482(2)
$CH^{79}BrF^{13}CF_3$	599.67(8)	−285.89(8)	−313.79(8)	0.0465(2)
$^{13}CH^{81}BrFCF_3$	501.31(9)	−238.86(8)	−262.45(8)	0.0471(2)
$CH^{81}BrF^{13}CF_3$	501.1(1)	−238.8(2)	−262.4(2)	0.0471(6)

[a] Asymmetry of the diagonalized χ tensor.$\eta = \frac{\chi_{xx} - \chi_{yy}}{\chi_{zz}}$

[b] Numbers in parentheses represent reported uncertainties and are given in units of the least significant digit. Reported numbers without parentheses were not reported with error.

method should not be followed. Secondly, P_{aa} is in good agreement to the similar structured CF_3CF_2Br [11], providing more evidence that the calculated structure is very similar to the experimental structure. Due to all of the evidence, then, of the agreement between the experimental and theoretical structure, the visual representation presented in Fig. 3 from the calculation is close enough to the experimental structure to be considered equivalent.

5.2. *Nuclear Quadrupole Coupling Tensor Comparisons*

The electronic structure environment is also of interest in order to understand the effects of different atomic substitutes to alkyl chains. This can be achieved by rotating the determined nuclear quadrupole coupling tensor from the principal axis system into a bromine-centered coordinate system. This has been done for all isotopologues and is reported in Table 8. Using the derived values, the asymmetry parameter, η, of the χ tensor was derived for each isotopologue. The determined values along with the η agree well with the theoretical values presented in Table 1, providing more evidence the theoretical structure is a good representation of the experimentally determined one.

In order to make some inferences about the effects of atomic substitutions on the experimental electronic structure, the determined χ_{zz} for the ^{79}Br of many similar bromine-containing small molecules have been compared to the determined value in this work. This comparison, along with the determined electric field gradient component, V_{zz}, is reported in Table 9. This value, coincident with the z-axis which is close to or lies along the C—Br bond for these species, is indicative of the covalency of the bond. A larger magnitude means more asymmetry at the nucleus and, therefore, indicates more electron sharing between the two species [46,47]. Electron withdrawing groups attached to carbon cause the atom to have a more positive charge and, since the bromine atom is rich in electron density, the value will increase due to more sharing of that electron density. The fluorines, being electron withdrawing groups, certainly have this effect on the bond as there is a very obvious jump in the observed V_{zz} value when moving from the hydrogenated alkanes to the fluorinated alkanes except for the initial fluorination of the bromomethane until the perfluorinated species is reached. A noticeable comparison in this work is the difference provided by taking away a singular fluorine and replacing it with a hydrogen from the previously studied bromoperfluoroethane [11]. This atomic substitution provides a 1.8% change in the value of V_{zz}. This is subtle, however, compared to the same substitution made between bromoperfluoromethane [40] and bromodifluoromethane [39]. This singular substitution produced an 8.8% change in the V_{zz} value and, thus, the covalency. Outside of the methyl species, however, the trend of fluorination of the alkane increasing the carbon-bromine covalency tends to be upheld and this work on 2-bromo-1,1,1,2-tetrafluoroethane reinforces that hypothesis. Further work on 2-bromo-1,1,1-trifluoroethane, however, is needed in order to provide more evidence in fully understanding this trend.

Table 9
Comparison of bromine-centered χ_{zz} values and electric field gradients of similar molecules.

Molecule	^{79}Br χ_{zz} /MHz	V_{zz}[a,b]	Reference
CH_3Br	573[c]	7.79	[34]
	578.847(48)[c]	7.87	[35]
CH_3CH_2Br	541	7.36	[29]
	537.5	7.31	[30]
$(CH_3)_2CHBr$	514.2(5)	6.99	[36]
g-$CH_3CH_2CH_2Br$	526.4	7.16	[37]
aa-$CH_3(CH_2)_2CH_2Br$	543.45(32)	7.39	[31]
CH_2FBr	554.52(38)	7.54	[38]
CHF_2Br	564.14(12)	7.67	[39]
CF_3Br	618.2(3)	8.41	[40]
CF_3CF_2Br	611.459(96)	8.31	[11]
CF_3CHFBr	599.88(3)	8.16	This Work
CF_3COCF_2Br	595.4(5)	8.10	[9]
trans-$CF_3CF_2CH_2Br$	620.839(7)	8.44	[10]

[d] Reported as eQq in the literature.

[e] Reported as eQq_{bond} in the literature.

[a] Electric field gradient is reported in atomic units. An atomic unit is E_h/ea_0^2 where E_h is the hartree, e is the charge on the electron, and a_0 is the Bohr.

[b] $V_{zz} = \chi_{zz}/(234.9647Q)$, where $\chi_{zz}$is in MHz and Q is 0.313 barn ($10^{-28}m^2$) as reported in Ref. [49].

[c] Numbers in parentheses represent reported uncertainties and are given in units of the least significant digit. Reported numbers without parentheses were not reported with error.

5.3. *Electric dipole forbidden, quadrupole allowed transitions*

Finally, the original thrust of this paper is to identify dipole forbidden, quadrupole allowed transitions in order to provide a basis in understanding their role in the planned M3WM experiments to be performed for chiral species testing. These are transitions containing $\Delta J \geq 2$ or are x-type transitions. The methods for identifying these transitions and their pathways have been discussed in previous literature of Grubbs and Cooke mentioned earlier and, therefore, will only be briefly commented on here. In this work, 19 such transitions were observed for the ^{79}Br and 26 were observed for the ^{81}Br.

In order to identify the pathways for quadrupole allowed transitions, it is necessary to utilize.egy files which can be created using tags in Pickett's program suite. To aid in the following discussion, the.egy file used here is provided in the Supplementary Material. As an example, we will use the $4_{1,4\frac{5}{2}} \leftarrow 2_{2,1\frac{3}{2}}$ transition of the parent ^{79}Br species from Fig. 1. In the fifth column of the.egy file is a value known as the P_{mix} coefficient. This term gives an effective purity of the state. The values for this coefficient lie between zero and unity. The closer to unity, the more pure the state. If we search the states involved in the transition, it is found that the P_{mix} coefficient value of the $2_{2,1\frac{3}{2}}$ state is 0.417652, or highly mixed. This mixing will be with a state of similar energy. The energy of the state is found in the third column of the.egy file, reported in wavenumbers. The reported energy of the state is 0.482582 cm^{-1}. Upon inspection, there is another state, the $3_{1,3\frac{3}{2}}$ state, at a very similar energy of 0.478645 cm^{-1} (118.028 MHz difference). Furthermore, this state also has a P_{mix} coefficient of 0.574930 indicating it, too, is highly mixed. The mixing of the two states, being coupled by a c-type tansition, is allowed through the large value of the χ_{ab} off-diagonal component. Because there is the observed, allowed a-type $4_{1,4\frac{5}{2}} \leftarrow 3_{1,3\frac{3}{2}}$ transition, the forbidden transition becomes enabled because the $\Delta F = \pm 1, 0$ selection rule is preserved.

Due to the chiral nature of the molecule producing all a-type, b-type, and c-type allowed species and the abundance of large off-diagonal components of the χ tensor, all three *a*-, *b*-, and *c*-type quadrupole allowed transitions were observed. In addition to this, however, the authors also observed multiple *x*-type transitions. *x*-type transitions of this type do not carry any change in parity of K_a or K_c, making the determination of the mixing states slightly more complex, but trackable. To the author's knowledge, we were the first to have observed this type of behavior in quadrupole allowed transitions and have attributed it to a pure breakdown in the *K*-labelling scheme of an asymmetric top [9]. With these identified, now we can test that theory along with the effects these transitions may or may not have in determining chiral enantiomers using M3WM experiments.

6. Conclusions

The microwave rotational spectrum of 2-bromo-1,1,1,2-tetrafluoroethane has been observed and reported for the first time on a CP-FTMW spectrometer. The recorded spectrum lies in the 6–18 GHz region of the electromagnetic spectrum. Six isotopologues, including ^{13}C isotopic substitution at each carbon atom in both the ^{79}Br and ^{81}Br parent species have been observed in natural abundance. All rotational constants, quartic centrifugal distortion contants, and nuclear quadrupole coupling tensor components have been experimentally determined and have been reported. In addition, spin-rotation components M_{aa}, M_{bb}, and M_{cc} are also determined and reported.

The theoretical structure of the molecule has been determined and is reported. In order to understand this structure and its congruence with the experimental structure, analysis of the experimentally determined structural parameters were undertaken. The positions of both carbons and the bromine have been fully determined using isotopic substitution. The C_1 position of the ^{79}Br could not be determined properly using single isotopic substitution so double substitution method of Rudolph [41] was leveraged in order to arrive at the reported position and agrees well with the single-substitution ^{81}Br structure. The resulting experimental structure is in excellent agreement with the theoretical structure allowing for it to be used interchangeably.

The electronic structure shows that there are large changes in the fluorination of the small brominated alkane species for the methyl derivatives but that this trend settles as the alkyl chain is lengthened but more work will need to be done on similar species in order to address the unknown gaps in these studies in order to reinforce the hypothesis that the C–Br bond, in general, strengthens as the molecule is fluorinated.

Lastly, a total of 45 electric dipole forbidden, quadrupole allowed transitions were observed for the title molecule inclusive of all four *a*-, *b*-, *c*-, and *x*-type transitions. All types of transitions will be used and tested in the planned M3WM experiments to be performed on these transitions in the near future.

Declaration of competing interest

The authors declare that they have no known competing financial interests or personal relationships that could have appeared to influence the work reported in this paper.

CRediT authorship contribution statement

Joshua E. Isert: Investigation, Formal analysis, Software. **Frank E. Marshall:** Investigation, Data curation. **William C. Bailey:** Resources, Formal analysis, Writing - review & editing. **G.S. Grubbs:** Conceptualization, Methodology, Software, Validation, Formal analysis, Writing - original draft, Supervision, Project administration, Funding acquisition.

Acknowledgements

The authors would like to thank the First Year Research Experiences (FYRE) Program of the College of Arts, Sciences, and Business (CASB) at Missouri S&T for providing the opportunity for JEI to get involved with this research through a small sponsorship. This material is based upon work supported by the National Science Foundation, United States under Grant No. CHE-1841346.

In recognition of this special edition of the *Journal of Molecular Structure* in memory of Jon Hougen, GSGII would like to acknowledge Jon's impact on his personal and professional life. Jon was a strong advocate of young people in science and GSGII was no different. He was very supportive and instructive to him with idea exchange, visits to the laboratory, and professional mentorship through phone conversations and e-mail. Jon's friendship as a scientist is something that forever has impacted GSGII and will be remembered as the cornerstone of their relationship. Along with his excellence as a scientist, this aspect of his life is one that many scientists share with Jon and will forever be noted in his legacy. He inspired GSGII to continue this legacy by asking him to "Do the same when you're in my position." A lesson GSGII will never forget nor dishonor.

Appendix A. Supplementary data

Supplementary data to this article can be found online at https://doi.org/10.1016/j.molstruc.2020.128277.

References

[1] D. Patterson, M. Schnell, J.M. Doyle, Nature 497 (2013) 475.
[2] S. Lobsiger, C. Perez, L. Evangelisti, K.K. Lehmann, B.H. Pate, J. Phys. Chem. Lett. 6 (2015) 196.
[3] V.A. Shubert, D. Schmitz, M. Schnell, J. Mol. Spectrosc. 300 (2014) 31.
[4] S. Eibenberger, J. Doyle, D. Patterson, Phys. Rev. Lett. 118 (2017) 123002.
[5] C.T. Dewberry, G.S. Grubbs II, S.A. Cooke, J. Mol. Spectrosc. 257 (2009) 66.
[6] G.S. Grubbs II, W.C. Bailey, S.A. Cooke, Chem. Phys. Lett. 477 (2009) 37.
[7] G.S. Grubbs II, W.C. Bailey, S.A. Cooke, Mol. Phys. 107 (2009) 2221.
[8] G.S. Grubbs II, S.A. Cooke, J. Mol. Struct. 963 (2010) 87.
[9] F.E. Marshall, D.J. Gillcrist, T.D. Persinger, S. Jaeger, C.C. Hurley, N.E. Shreve, N. Moon, G.S. Grubbs II, J. Mol. Spectrosc. 328 (2016) 59.
[10] F.E. Marshall, N. Moon, T.D. Persinger, D.J. Gillcrist, N.E. Shreve, W.C. Bailey, G.S. Grubbs II, High resolution spectroscopy near the continuum limit: the microwave spectrum of trans-3-bromo-1,1,1,2,2-pentafluoropropane, Mol. Phys. 117 (2019) 1351–1359.
[11] B.E. Long, G.S. Grubbs II, J.D. Langridge, S.A. Cooke, J. Mol. Struct. 1023 (2012) 55.
[12] A. Javan, Phys. Rev. 107 (1957) 1579.
[13] T. Oka, J. Chem. Phys. 45 (1966) 752.
[14] F.E. Marshall, R. Dorris, S.A. Peebles, R.A. Peebles, G.S. Grubbs II, J. Phys. Chem. A 122 (2018) 7385.
[15] Z. Kisiel, J. Kosarzewski, Acta Phys. Pol. 131 (2017) 311.
[16] M.J. Frisch, G.W. Trucks, H.B. Schlegel, G.E. Scuseria, M.A. Robb, J.R. Cheeseman, G. Scalmani, V. Barone, B. Mennucci, G.A. Petersson, H. Nakatsuji, M. Caricato, X. Li, H.P. Hratchian, A.F. Izmaylov, J. Bloino, G. Zheng, J.L. Sonnenberg, M. Hada, M. Ehara, R.F.K. Toyota, J. Hasegawa, M. Ishida, T. Nakajima, Y. Honda, O. Kitao, H. Nakai, T. Vreven, J.A. Montgomery Jr., J.E. Peralta, F. Ogliaro, M. Bearpark, J.J. Heyd, K.N.K.E. Brothers, V.N. Staroverov, R. Kobayashi, J. Normand, K. Raghavachari, A. Rendell, J.C. Burant, S.S. Iyengar, J. Tomasi, M. Cossi, N. Rega, J.M. Millam, M. Klene, J.E. Knox, J.B. Cross, V. Bakken, C. Adamo, J. Jaramillo, R. Gomperts, R.E. Stratmann, O. Yazyev, A.J. Austin, R. Cammi, C. Pomelli, J.W. Ochterski, R.L. Martin, K. Morokuma, V.G. Zakrzewski, G.A. Voth, P. Salvador, J.J. Dannenberg, S. Dapprich, A.D. Daniels, O. Farkas, J.B. Foresman, J.V. Ortiz, J. Cioslowski, D.J. Fox, Gaussian 09, Revision D.01, 06492, Gaussian, Inc., 340 Quinnipiac Street, Building 40, Wallingford, CT, 2009. copyright © 1994-2009.
[17] W.C. Bailey, F.M. Gonzalez, J. Mol. Struct. 651–653 (2002) 689.
[18] A.D. Becke, J. Chem. Phys. 104 (1996) 1040.
[19] C. Adamo, V. Barone, Chem. Phys. Lett. 274 (1977) 242.
[20] A. Schäfer, J. Chem. Phys. 100 (1994) 5829.
[21] D. Feller, J. Comput. Chem. 17 (1996) 1571.
[22] K.L. Schuchardt, B.T. Didier, T. Elsethagen, L. Sun, V. Gurumoorthi, J. Chase, J. Li, T.L. Windus, J. Chem. Inf. Model. 47 (2007) 1045.
[23] W.C. Bailey, Calculation of Nuclear Quadrupole Coupling Constants in Gaseous State Molecules, 2018. http://web.mac.com/wcbailey/nqcc/.

[24] H.M. Pickett, J. Mol. Spectrosc. 148 (1991) 371.
[25] Z. Kisiel, L. Pszczółkowski, I.R. Medvedev, M. Winnewisser, F.C.D. Lucia, C.E. Herbst, J. Mol. Spectrosc. 233 (2005) 231.
[26] Z. Kisiel, PROSPE – Programs for ROtational SPEctroscopy, 2019. http://info.ifpan.edu.pl/kisiel/prospe.htm.
[27] Z. Kisiel, Spectroscopy from Space, Kluwer Academic Publishers, Dordrecht, 2001.
[28] J.K.G. Watson, Vibrational Spectra and Structure, vol. 6, Elsevier, Amsterdam, 1977.
[29] C. Flanagan, L. Pierce, J. Chem. Phys. 38 (1963) 2963.
[30] R.S. Wagner, B.P. Dailey, N. Solimene, J. Chem. Phys. 26 (1957) 1593.
[31] J. Kim, H. Jang, S. Ka, D.A. Obenchain, R.A. Peebles, S.A. Peebles, J.J. Oh, J. Mol. Spectrosc. 328 (2016) 50.
[32] J.A. Fournier, R.K. Bohn, J.A. Montgomery Jr., M. Onda, J. Phys. Chem. A 114 (2010) 1118–1122.
[33] J.A. Fournier, R.K. Bohn, Dalton Trans. 39 (2010) 4575–4578.
[34] W. Gordy, J.W. Simmons, A. Smith, Phys. Rev. 72 (1947) 344.
[35] J. Dubrulle, J. Burie, D. Boucher, F. Herelemont, J. Demaison, J. Mol. Spectrosc. 88 (1981) 394.
[36] R.H. Schwendeman, F.L. Tobiason, J. Chem. Phys. 43 (1965) 201.
[37] Y. Niide, I. Ohkoshi, M. Takano, J. Mol. Spectrosc. 89 (1981) 387.
[38] A. Baldacci, P. Stoppa, A.P. Charmet, S. Giorgianni, G. Cazzoli, C. Puzzarini, R. Larsen, J. Phys. Chem. A 111 (2007) 7090.
[39] G. Cazzoli, L. Cludi, C. Puzzarini, P. Stoppa, A.P. Charmet, N. Tasinato, A. Baldacci, A. Baldan, S. Giorgianni, R.W. Larsen, S. Stopkowicz, J. Gauss, J. Phys. Chem. A 115 (2011) 453.
[40] A.P. Cox, G. Duxbury, J.A. Hardy, Y. Kawashima, J. Chem. Soc., Faraday Trans. 2 (76) (1980) 339.
[41] H.D. Rudolph, J. Mol. Spectrosc. 89 (1981) 430–439.
[42] J. Kraitchman, Am. J. Phys. 21 (1953) 17.
[43] J.K.G. Watson, A. Roytburg, W. Ulrich, J. Mol. Spectrosc. 196 (1999) 102.
[44] Z. Kisiel, J. Mol. Spectrosc. 218 (2003) 58.
[45] R.K. Bohn, J.A. Montgomery Jr., H.H. Michels, J.A. Fournier, J. Mol. Spectrosc. 325 (2016) 42.
[46] C.H. Townes, B.P. Dailey, J. Chem. Phys. 17 (1949) 782.
[47] W. Gordy, R.L. Cook, Microwave Molecular Spectra, in: Techniques of Chemistry, vol. XVIII, Wiley, New York, 1984.
[48] C.C. Costain, Trans. Am. Cryst. Assoc. 2 (1966) 157.
[49] P. Pyykkö, Mol. Phys. 106 (2008) 1965.